



Crystal structure and characterization of magnesium carbonate chloride heptahydrate

Christine Rincke,^{a*} Horst Schmidt,^a Gernot Buth^b and Wolfgang Voigt^a

^aInstitute of Inorganic Chemistry, TU Bergakademie Freiberg, Leipziger Strasse 29, D-09599 Freiberg, Germany, and ^bInstitute for Photon Science and Synchrotron Radiation (IPS), Karlsruhe Institute of Technology (KIT), Hermann-von-Helmholtz-Platz 1, D-76344 Eggenstein-Leopoldshafen, Germany. *Correspondence e-mail: christine.rincke@chemie.tu-freiberg.de

Received 24 March 2020

Accepted 19 June 2020

Edited by H. Uekusa, Tokyo Institute of Technology, Japan

Keywords: magnesium; carbonate; chloride; hydrate; synchrotron; twinning; crystal structure.

CCDC reference: 2010753

Supporting information: this article has supporting information at journals.iucr.org/c

$\text{MgCO}_3 \cdot \text{MgCl}_2 \cdot 7\text{H}_2\text{O}$ is the only known neutral magnesium carbonate containing chloride ions at ambient conditions. According to the literature, only small and twinned crystals of this double salt could be synthesised in a concentrated solution of MgCl_2 . For the crystal structure solution, single-crystal diffraction was carried out at a synchrotron radiation source. The monoclinic crystal structure (space group Cc) exhibits double chains of MgO octahedra linked by corners, connected by carbonate units and water molecules. The chloride ions are positioned between these double chains parallel to the (100) plane. Dry $\text{MgCO}_3 \cdot \text{MgCl}_2 \cdot 7\text{H}_2\text{O}$ decomposes in the air to chlorartinite, $\text{Mg}_2(\text{OH})\text{Cl}(\text{CO}_3) \cdot n\text{H}_2\text{O}$ ($n = 2$ or 3). This work includes an extensive characterization of the title compound by powder X-ray diffraction, thermal analysis, SEM and vibrational spectroscopy.

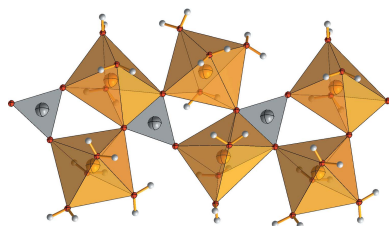
1. Introduction

In the context of CO_2 research, the interactions of CO_2 with salts and brine solutions are of great interest. Therefore, the system MgCl_2 – MgCO_3 – H_2O – CO_2 has been investigated. The only nonbasic salt containing carbonate and chloride ions is $\text{MgCO}_3 \cdot \text{MgCl}_2 \cdot 7\text{H}_2\text{O}$ (Rincke, 2018).

The formation conditions of $\text{MgCO}_3 \cdot \text{MgCl}_2 \cdot 7\text{H}_2\text{O}$ were described for the first time by Gloss (1937) and Walter-Levy (1937). It can be synthesized at room temperature by adding $\text{MgCO}_3 \cdot 3\text{H}_2\text{O}$ to a highly concentrated solution of magnesium chloride saturated with CO_2 (Gloss, 1937; Schmidt, 1960).

Within the scope of outbursts of CO_2 in potash mines, $\text{MgCO}_3 \cdot \text{MgCl}_2 \cdot 7\text{H}_2\text{O}$ was discussed as a storage compound for CO_2 in the 1960s (Schmidt, 1960; Serowy, 1963; Serowy & Liebmann, 1964; Schmittler, 1964; D'Ans, 1967). This salt forms needle-like crystals, which are only stable in concentrated MgCl_2 solution (Moshkina & Yaroslavtseva, 1970). It decomposes immediately when it is washed with water. When it was stored in air, basic carbonate was formed (Gloss, 1937).

Schmittler (1964) concluded from a powder X-ray diffraction (PXRD) pattern of $\text{MgCO}_3 \cdot \text{MgCl}_2 \cdot 7\text{H}_2\text{O}$ that its crystal structure exhibits a C -centred monoclinic lattice with parameters $a = 13.27$ (0), $b = 11.30$ (8), $c = 9.22$ (7) Å and $\beta = 118.2$ (6)°. Due to the low scattering power and the small size of the crystals, a crystal structure analysis of single crystals was not possible until now. Our own investigations should provide a better comprehension of the synthesis of $\text{MgCO}_3 \cdot \text{MgCl}_2 \cdot 7\text{H}_2\text{O}$ and provide a more detailed characterization, including a crystal structure analysis.



OPEN ACCESS

2. Experimental

2.1. Synthesis and crystallization

The synthesis of $\text{MgCO}_3 \cdot \text{MgCl}_2 \cdot 7\text{H}_2\text{O}$ is based on the information of Schmidt (1960). MgO (1 g, Magnesia M2329, p.a.) was added to 200 g of an aqueous solution of MgCl_2 (5.5 molal, Fluka, $\geq 98\%$). The suspension was stirred for 30 min. Afterwards, the undissolved MgO was filtered off. CO_2 was bubbled through the stirred solution for 24 h at room temperature. The product was filtered off for further characterization.

2.2. Single-crystal diffraction

Data were collected on beamline SCD at the KIT Synchrotron Radiation Source using a Stoe IPDS diffractometer with monochromated radiation of $\lambda = 0.8000 \text{ \AA}$. A crystal of $\text{MgCO}_3 \cdot \text{MgCl}_2 \cdot 7\text{H}_2\text{O}$ was recovered from a droplet of its mother liquor and mounted rapidly in the cold (150 K) stream of nitrogen gas of the diffractometer.

2.3. Powder X-ray diffraction (PXRD)

PXRD patterns were taken for phase identification with a laboratory Bruker D8 Discover powder diffractometer in Bragg–Brentano set up ($\text{Cu } K\alpha_1$ radiation, Vantec 1 detector). The samples were prepared as flat plates and measured at room temperature.

2.4. Thermal analysis

The thermal analysis was performed with a TG/DTA 220 instrument from Seiko Instruments (reference substance: Al_2O_3 , open platinum crucible; argon flow: 300 ml min^{-1} ;

Table 1

Experimental details.

Crystal data	
Chemical formula	$\text{MgCO}_3 \cdot \text{MgCl}_2 \cdot 7\text{H}_2\text{O}$
M_r	305.64
Crystal system, space group	Monoclinic, Cc
Temperature (K)	150
a, b, c (Å)	13.368 (5), 11.262 (5), 9.266 (4)
β (°)	118.83 (3)
V (Å ³)	1222.0 (9)
Z	4
Radiation type	Synchrotron, $\lambda = 0.8000 \text{ \AA}$
μ (mm ⁻¹)	0.93
Crystal size (mm)	$0.13 \times 0.07 \times 0.01 \times 0.02$ (radius)
Data collection	
Diffractometer	Stoe IPDS II
Absorption correction	For a sphere (Coppens, 1970)
No. of measured, independent and observed [$I > 2\sigma(I)$] reflections	8746, 6975, 5476
R_{int}	0.0613
θ_{max} (°)	26.7
$(\sin \theta/\lambda)_{\text{max}}$ (Å ⁻¹)	0.561
Refinement	
$R[F^2 > 2\sigma(F^2)], wR(F^2), S$	0.053, 0.161, 1.12
No. of reflections	4791
No. of parameters	179
No. of restraints	22
H-atom treatment	Only H-atom coordinates refined
$\Delta\rho_{\text{max}}, \Delta\rho_{\text{min}}$ (e Å ⁻³)	0.36, -0.43
Absolute structure	Flack x determined using 647 quotients $[(I^+) - (I^-)] / [(I^+) + (I^-)]$ (Parsons <i>et al.</i> , 2013)
Absolute structure parameter	0.43 (13)

Computer programs: X-Area (Stoe & Cie, 2015), X-RED (Stoe & Cie, 2015), SHELXS97 (Sheldrick, 2008), SHELXL2016 (Sheldrick, 2015), DIAMOND (Brandenburg, 2017) and publCIF (Westrip, 2010).

heating rate: 5 K min^{-1} , prior period 30 min at 298.15 K in an argon flow).

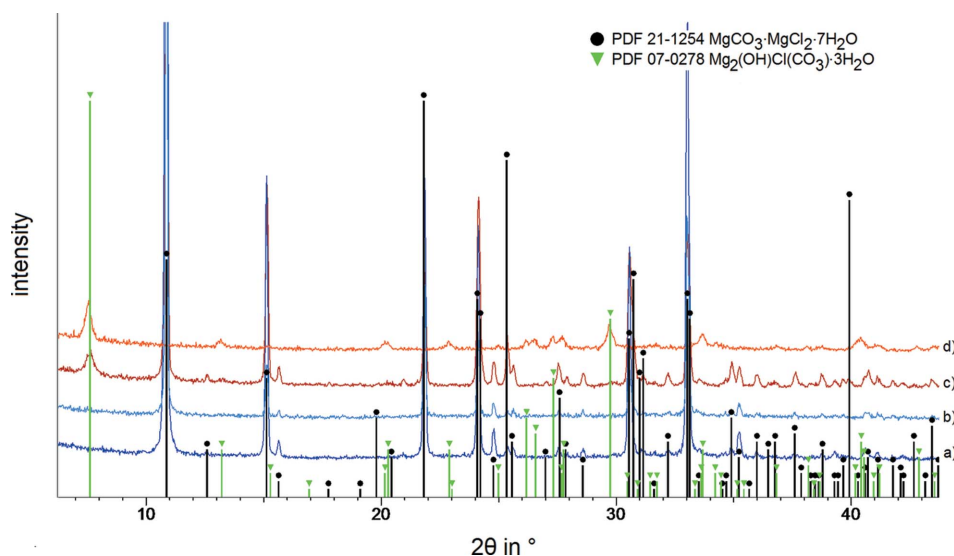


Figure 1

Powder XRD patterns of $\text{MgCO}_3 \cdot \text{MgCl}_2 \cdot 7\text{H}_2\text{O}$ under ambient conditions ($\text{Cu } K\alpha_1$ radiation) for (a) the unwashed product immediately after the synthesis, (b) the unwashed product stored in the air after 19 months, (c) the product washed with ethanol after storage in the air for 10 d and (d) the product washed with ethanol after storage in the air for 19 months. Reference data: $\text{MgCO}_3 \cdot \text{MgCl}_2 \cdot 7\text{H}_2\text{O}$ (PDF 21-1254) and $\text{Mg}_2(\text{OH})\text{Cl}(\text{CO}_3) \cdot 3\text{H}_2\text{O}$ (PDF 07-0278).

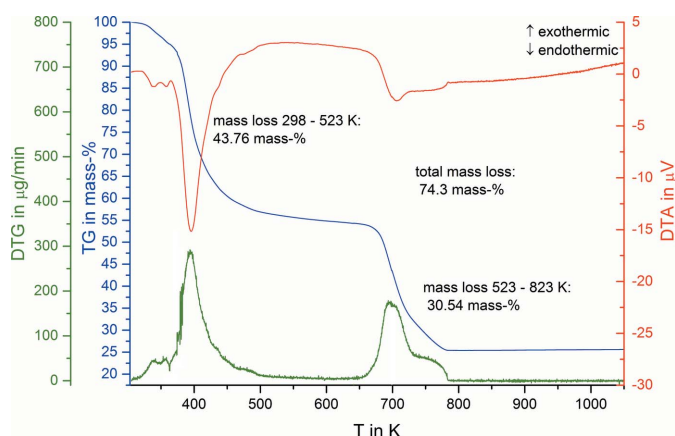


Figure 2
Thermal analysis of $\text{MgCO}_3\cdot\text{MgCl}_2\cdot 7\text{H}_2\text{O}$.

2.5. Scanning electron microscopy (SEM)

The SEM images were recorded with a TESCAN Vega 5130 SB instrument (20 kV accelerating voltage). The sample was coated with gold.

2.6. Vibrational spectroscopy

For the FT-IR spectrum, a Thermo Scientific Nicolet 380 FTIR spectrometer (spectral resolution: 6 cm^{-1} , 256 scans per measurement) with KBr blanks was used.

The Raman spectrum was recorded shortly after synthesis with a Bruker RFS100/S FT spectrometer at room temperature (Nd/YAG-laser, wavelength of the laser: 1064 nm).

2.7. Refinement

Crystal data, data collection and structure refinement details are given in Table 1. Due to the small crystals and their low scattering power, the crystal structure solution was carried out by single-crystal diffraction at a synchrotron radiation source. The quality of the crystals affected the measured data set with the effect that only reflections to $\sin \theta_{\text{max}}/\lambda = 0.56\text{ \AA}^{-1}$ could be considered for the structure refinement. The crystal structure was solved by direct methods. The resulting structure solution exhibits a chemically reasonable atomic arrangement, distances, angles and displacement parameters.

H atoms were placed in the positions indexed by difference Fourier maps and their U_{iso} values were set at $1.2U_{\text{eq}}(\text{O})$ using a riding-model approximation.

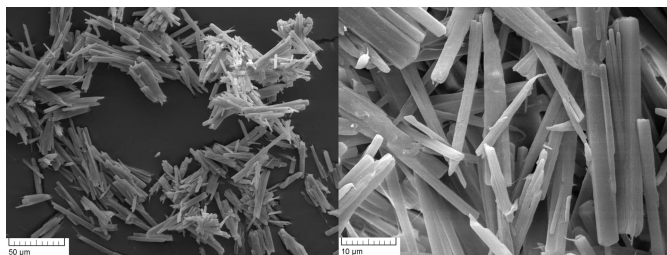


Figure 3
SEM images of $\text{MgCO}_3\cdot\text{MgCl}_2\cdot 7\text{H}_2\text{O}$, with the crystals exhibiting twinning or even further intergrowth.

Table 2

Assignment of the IR and Raman bands of $\text{MgCO}_3\cdot\text{MgCl}_2\cdot 7\text{H}_2\text{O}$.

IR	Raman	Assignment (Coleyshaw <i>et al.</i> , 2003)
3407, 3240	3386, 3250	$\nu(\text{OH})_{\text{W}}$
1635	1660	$\delta(\text{OH})_{\text{W}}$
1550, 1449, 1401	1544	$\nu_{\text{as}}(\text{CO})$
1114	1111	$\nu_{\text{s}}(\text{CO})$
845	794	$\gamma(\text{CO})$
620	599	$\delta_{\text{as}}(\text{CO})$
457	403, 227, 181, 154, 124	lattice vibrations

Notes: ν = valence vibration, δ = deformation vibration (in the plane), γ = deformation vibration out of the plane, W = water, s = symmetric and as = asymmetric.

The crystal exhibits nonmerohedral twinning. The matrix that relates the individual diffraction pattern was determined as $(1\ 0\ 1.38, 0\ -1\ 0, 0\ 0\ -1)$. The reflections of both domains were integrated (number of reflections in domain 1: 2829; domain 2: 3505; overlaid: 641; major twin component fraction: 56.45%).

3. Results and discussion

3.1. Characterization of magnesium carbonate chloride heptahydrate

The characterization of the unwashed product with PXRD is in accordance with the reference pattern PDF 21-1254 for $\text{MgCO}_3\cdot\text{MgCl}_2\cdot 7\text{H}_2\text{O}$ (Schmittler, 1964). The filtered product was stored in a sealed vessel. After 19 months, the powder pattern remained constant, *i.e.* the product did not alter. If the product was washed with ethanol and stored in the air, decomposition to chlorartinite [$\text{Mg}_2(\text{OH})\text{Cl}(\text{CO}_3)\cdot 3\text{H}_2\text{O}$] begins within a few days (Fig. 1). This observation confirms the information of Gloss (1937).

The thermal decomposition of $\text{MgCO}_3\cdot\text{MgCl}_2\cdot 7\text{H}_2\text{O}$ starts as early as the heating begins and shows two main steps (Fig. 2). H_2O , CO_2 and HCl are evaporated off. This is in accordance with the observation of Serowy & Liebmann (1964). A precise assignment of the stepwise mass loss is not possible. The characterization of the residue with PXRD at 573 K exhibits the presence of a mixture of basic magnesium carbonates, *i.e.* hydromagnesite [$\text{Mg}_5(\text{CO}_3)_4(\text{OH})_2\cdot 4\text{H}_2\text{O}$] and amorphous phases. At 803 K the decomposition is complete and only MgO remains in the residue. The observed mass loss of 74.3 (1)% confirms the theoretical mass loss of 73.6%.

The SEM images of $\text{MgCO}_3\cdot\text{MgCl}_2\cdot 7\text{H}_2\text{O}$ show thin needles ($50 \times 5\ \mu\text{m}$), which are twinned or even more intergrown (Fig. 3). Numerous crystallization experiments with the aim of obtaining larger crystals were not successful.

The FT-IR (Fig. 4) and Raman spectra (Fig. 5) of $\text{MgCO}_3\cdot\text{MgCl}_2\cdot 7\text{H}_2\text{O}$ confirm the absence of hydroxide ions in the crystal structure, because there are no bands above 3500 cm^{-1} as in chlorartinite, $\text{Mg}_2(\text{OH})\text{Cl}(\text{CO}_3)\cdot 3\text{H}_2\text{O}$ (Vergasova *et al.*, 1998). The assignment of the bands was concluded from a comparison with the vibrational spectra of other neutral magnesium carbonates and chlorartinite (Coleyshaw *et al.*, 2003; Vergasova *et al.*, 1998) (Table 2).

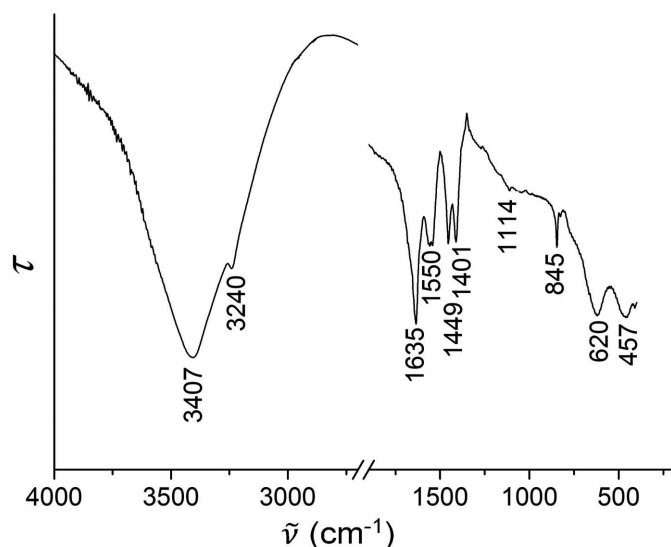


Figure 4 IR spectrum of $\text{MgCO}_3 \cdot \text{MgCl}_2 \cdot 7\text{H}_2\text{O}$ under ambient conditions.

3.2. Crystal structure of magnesium carbonate chloride heptahydrate

The monoclinic crystal structure of $\text{MgCO}_3 \cdot \text{MgCl}_2 \cdot 7\text{H}_2\text{O}$ with the space group Cc and the lattice parameters published by Schmittler (1964) were confirmed. There are two distinguishable magnesium ions. Mg1 is coordinated by three water molecules and two carbonate anions. One carbonate acts as a monodentate ligand *via* atom O9 and the other as a bidentate ligand *via* atoms O2 and O6 . The octahedra of Mg2 are formed by four water molecules and two carbonate units which are connected to the magnesium ion in a monodentate manner *via* atoms O2 and O6 (Fig. 6). The corner-linked Mg-O octahedra are arranged in a zigzag manner and together with the carbonate units form double chains parallel to the (100) plane (Fig. 7).

All the carbonate units are crystallographically equivalent and exhibit a C_s geometry, because they are planar, but the C-O bonds have different lengths. Each carbonate unit is coordinated by three magnesium ions: monodentate to Mg1 ,

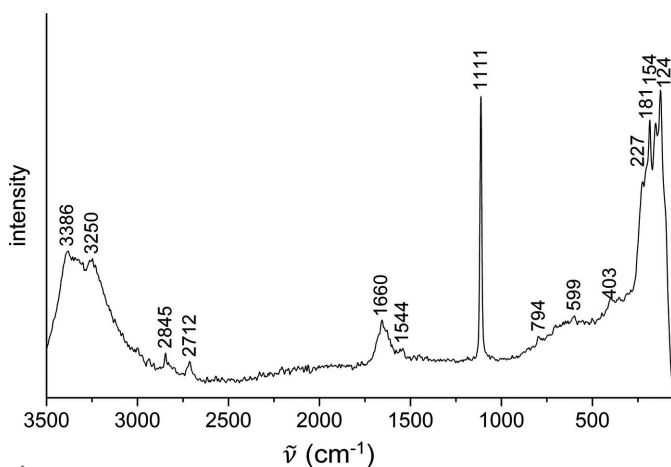


Figure 5 Raman spectrum of $\text{MgCO}_3 \cdot \text{MgCl}_2 \cdot 7\text{H}_2\text{O}$ under ambient conditions.

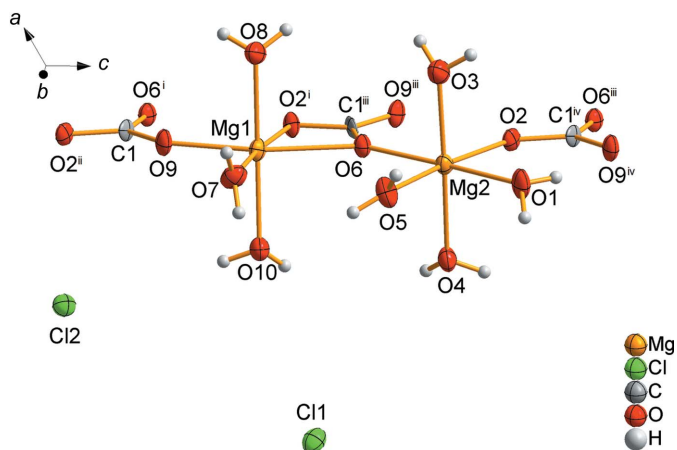


Figure 6 The asymmetric unit and coordination units of $\text{MgCO}_3 \cdot \text{MgCl}_2 \cdot 7\text{H}_2\text{O}$ [symmetry codes: (i) $x, -y, z - \frac{1}{2}$; (ii) $x, y, z - 1$; (iii) $x, -y, z + \frac{1}{2}$; (iv) $x, y, z + 1$].

bidentate to Mg1^i and monodentate to Mg2^{ii} (see Fig. 6 for symmetry codes). In addition, the carbonate units stabilize the double chains (Fig. 7).

Between the double chains, which are arranged in a zigzag-like stacking order parallel to the (001) plane, are located the chloride ions Cl1 and Cl2 (Fig. 8). The positions of atoms H1A and H3B are fixed by short hydrogen bonds to atoms O9^{iv} and O4^{vi} , and the other H atoms by interactions with the chloride ions (Table 3 and Fig. 9). As a consequence, a three-dimensional network is formed.

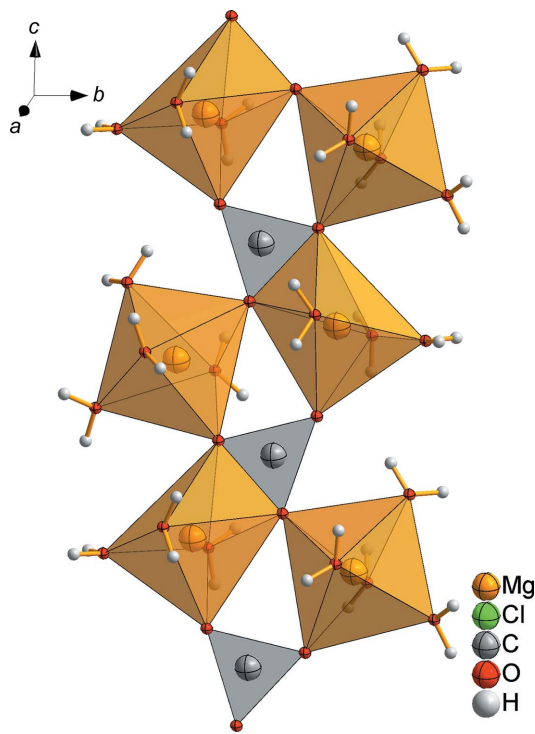


Figure 7 The characteristic structural motif in $\text{MgCO}_3 \cdot \text{MgCl}_2 \cdot 7\text{H}_2\text{O}$, showing the double chain of MgO octahedra linked by corners and carbonate units parallel to the (100) plane.

Table 3
Hydrogen-bond geometry (Å, °).

$D-H\cdots A$	$D-H$	$H\cdots A$	$D\cdots A$	$D-H\cdots A$
O1—H1A \cdots O9 ^{iv}	0.82 (3)	1.94 (6)	2.688 (14)	153 (13)
O1—H1B \cdots Cl2 ^{iv}	0.82 (3)	2.38 (4)	3.186 (11)	167 (12)
O3—H3A \cdots Cl2 ^v	0.82 (3)	2.32 (3)	3.135 (11)	174 (17)
O3—H3B \cdots O4 ^{vi}	0.82 (3)	2.10 (11)	2.796 (13)	143 (17)
O4—H4A \cdots Cl1 ^{vii}	0.82 (3)	2.36 (3)	3.176 (10)	171 (14)
O4—H4B \cdots Cl1 ^{viii}	0.82 (3)	2.49 (7)	3.251 (10)	155 (13)
O5—H5A \cdots Cl2 ^{viii}	0.82 (3)	2.45 (7)	3.222 (11)	157 (16)
O5—H5B \cdots Cl1 ^{ix}	0.81 (3)	2.54 (6)	3.327 (11)	164 (17)
O7—H7A \cdots Cl2 ^{viii}	0.82 (3)	2.42 (6)	3.212 (11)	163 (16)
O7—H7B \cdots Cl1 ^x	0.82 (3)	2.30 (4)	3.111 (11)	169 (16)
O8—H8A \cdots Cl2 ^{vi}	0.82 (3)	2.46 (5)	3.254 (10)	163 (11)
O8—H8B \cdots Cl2 ^v	0.82 (3)	2.41 (3)	3.233 (10)	178 (11)
O10—H10A \cdots Cl1 ^{viii}	0.82 (3)	2.34 (5)	3.146 (10)	166 (15)
O10—H10B \cdots Cl1 ^{xi}	0.82 (3)	2.67 (7)	3.424 (10)	154 (12)

Symmetry codes: (iv) $x, y, z + 1$; (v) $x + \frac{1}{2}, y - \frac{1}{2}, z + 1$; (vi) $x + \frac{1}{2}, -y + \frac{1}{2}, z + \frac{1}{2}$; (vii) $x, y - 1, z$; (viii) $x, -y + 1, z + \frac{1}{2}$; (ix) $x + \frac{1}{2}, -y + \frac{3}{2}, z + \frac{1}{2}$; (x) $x + \frac{1}{2}, y - \frac{1}{2}, z$; (xi) $x, -y + 1, z - \frac{1}{2}$.

The structural motifs of such double chains are similar in $MgCO_3 \cdot MgCl_2 \cdot 7H_2O$ and $MgCO_3 \cdot 3H_2O$ (Giester *et al.*, 2000), but in contrast to $MgCO_3 \cdot 3H_2O$ in $MgCO_3 \cdot MgCl_2 \cdot 7H_2O$, only two of three carbonate units and three and four water molecules instead of two water molecules are linked to each Mg atom. Furthermore, no free water molecules are positioned between these double chains in $MgCO_3 \cdot MgCl_2 \cdot 7H_2O$. The crystal structures of other neutral magnesium carbonates, *e.g.* $MgCO_3 \cdot 5H_2O$, $MgCO_3 \cdot 6H_2O$ and the chloride-containing magnesium carbonates $Mg_2(OH)Cl(CO_3) \cdot 2H_2O$ (chlorartinite) and $Mg_2(OH)Cl(CO_3) \cdot H_2O$ (dehydrated clorartinite), do not exhibit such double chains (Liu *et al.*, 1990; Rincke *et al.*, 2020; Sugimoto *et al.*, 2006, 2007). Therefore, the crystal structure of $MgCO_3 \cdot MgCl_2 \cdot 7H_2O$ is unique.

Acknowledgements

The award of synchrotron beamtime at KIT Synchrotron Radiation Source, Karlsruhe, Germany, is gratefully acknowledged.

References

Brandenburg, K. (2017). *DIAMOND*. Crystal Impact GbR, Bonn, Germany.
 Coleyshaw, E. E., Crump, G. & Griffith, W. P. (2003). *Spectrochim. Acta A Mol. Biomol. Spectrosc.* **59**, 2231–2239.
 Coppens, P. (1970). *Crystallographic Computing*, edited by F. R. Ahmed, S. R. Hall & C. P. Huber, pp. 255–270. Copenhagen: Munksgaard.
 D'Ans, J. (1967). *Kali und Steinsalz*, **4**, 396–401.
 Giester, G., Lengauer, C. L. & Rieck, B. (2000). *Mineral. Petrol.* **70**, 153–163.
 Gloss, G. (1937). Dissertation. Friedrich-Wilhelms-University of Berlin, Germany.
 Liu, B., Zhou, X., Cui, X. & Tang, J. (1990). *Sci. China Ser. B*, **33**, 1350–1356.
 Moshkina, I. A. & Yaroslavtseva, L. M. (1970). *Zh. Neorg. Khim.* **15**, 3345–3350.
 Parsons, S., Flack, H. D. & Wagner, T. (2013). *Acta Cryst.* **B69**, 249–259.
 Rincke, C. (2018). Dissertation. TU Bergakademie Freiberg, Germany.

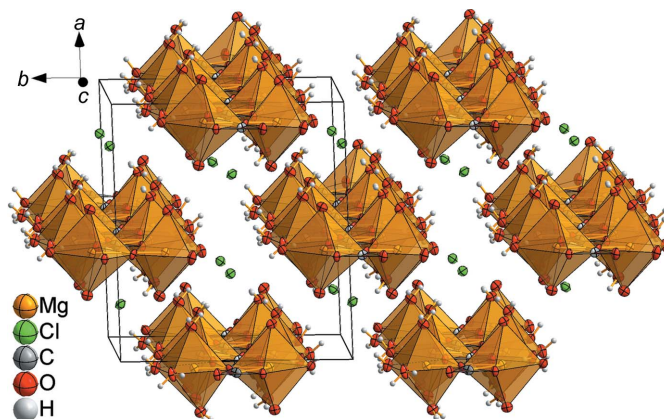


Figure 8
Excerpt of the crystal structure of $MgCO_3 \cdot MgCl_2 \cdot 7H_2O$, showing the zigzag-like stacking order of the double chains and the chloride ions between them.

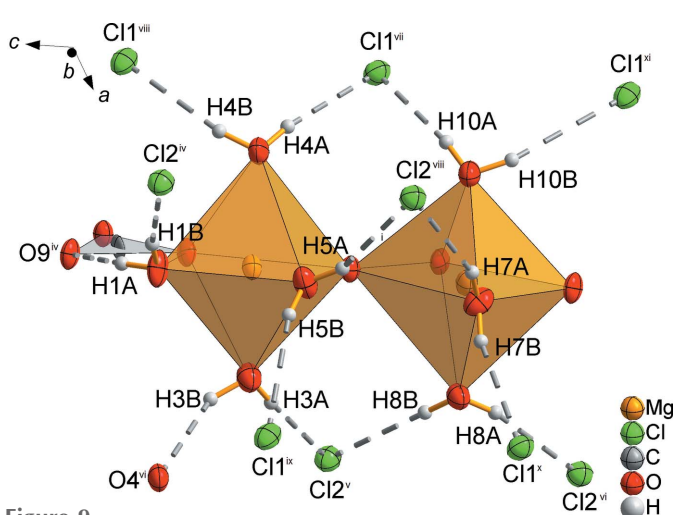


Figure 9
Excerpt of the crystal structure of $MgCO_3 \cdot MgCl_2 \cdot 7H_2O$, showing the hydrogen-bond interactions of the H atoms with chloride ions (dashed lines) [symmetry codes: (iv) $x, y, z + 1$; (v) $x + \frac{1}{2}, y - \frac{1}{2}, z + 1$; (vi) $x + \frac{1}{2}, -y + \frac{1}{2}, z + \frac{1}{2}$; (vii) $x, y - 1, z$; (viii) $x, -y + 1, z + \frac{1}{2}$; (ix) $x + \frac{1}{2}, -y + \frac{3}{2}, z + \frac{1}{2}$; (x) $x + \frac{1}{2}, y - \frac{1}{2}, z$; (xi) $x, -y + 1, z - \frac{1}{2}$].

Rincke, C., Schmidt, H. & Voigt, W. (2020). *Acta Cryst.* **C76**, 244–249.
 Schmidt, E. (1960). *Bergakademie*, **12**, 693–697.
 Schmittler, H. (1964). *Deut. Akad. Wiss.* **6**, 644–648.
 Serowy, F. (1963). *Freiberger Forschungshefte A*, **267**, 405–419.
 Serowy, F. & Liebmann, G. (1964). *Wissenschaftl. Zeitschrift der Technischen Hochschule für Chemie 'Carl Schorlemmer' Leuna-Merseburg*, **6**, 338–342.
 Sheldrick, G. M. (2008). *Acta Cryst.* **A64**, 112–122.
 Sheldrick, G. M. (2015). *Acta Cryst.* **C71**, 3–8.
 Stoe & Cie (2015). *X-Area and X-Red32*. Stoe & Cie, Darmstadt, Germany.
 Sugimoto, K., Dinnebier, R. E. & Schlecht, T. (2006). *J. Appl. Cryst.* **39**, 739–744.
 Sugimoto, K., Dinnebier, R. E. & Schlecht, T. (2007). *Powder Diff.* **22(1)**, 739–744.
 Vergasova, L. P., Filation, S. K., Serafimova, E. K. & Sergeeva, S. V. (1998). *Zapiski Vserossiiskogo Mineralogicheskogo Obshchestva*, **127**, 55–59.
 Walter-Levy, L. (1937). *Compt. Rend.* **205**, 1405–1407.
 Westrip, S. P. (2010). *J. Appl. Cryst.* **43**, 920–925.

supporting information

Acta Cryst. (2020). C76, 741-745 [https://doi.org/10.1107/S2053229620008153]

Crystal structure and characterization of magnesium carbonate chloride heptahydrate

Christine Rincke, Horst Schmidt, Gernot Buth and Wolfgang Voigt

Computing details

Data collection: *X-AREA* (Stoe & Cie, 2015); cell refinement: *X-AREA* (Stoe & Cie, 2015); data reduction: *X-RED* (Stoe & Cie, 2015); program(s) used to solve structure: *SHELXS97* (Sheldrick, 2008); program(s) used to refine structure: *SHELXL2016* (Sheldrick, 2015); molecular graphics: *DIAMOND* (Brandenburg, 2017); software used to prepare material for publication: *publCIF* (Westrip, 2010).

Magnesium carbonate chloride heptahydrate

Crystal data

MgCO₃·MgCl₂·7H₂O

$M_r = 305.64$

Monoclinic, *Cc*

$a = 13.368$ (5) Å

$b = 11.262$ (5) Å

$c = 9.266$ (4) Å

$\beta = 118.83$ (3)°

$V = 1222.0$ (9) Å³

$Z = 4$

$F(000) = 632$

$D_x = 1.661$ Mg m⁻³

Synchrotron radiation, $\lambda = 0.8000$ Å

Cell parameters from 4192 reflections

$\theta = 2.7$ – 29.5 °

$\mu = 0.93$ mm⁻¹

$T = 150$ K

Needle, colourless

$0.13 \times 0.07 \times 0.01 \times 0.02$ (radius) mm

Data collection

Stoe IPDS II

diffractometer

Radiation source: synchrotron

rotation method scans

Absorption correction: for a sphere

(Coppens, 1970)

6975 independent reflections

5476 reflections with $I > 2\sigma(I)$

$R_{\text{int}} = 0.061$

$\theta_{\text{max}} = 26.7$ °, $\theta_{\text{min}} = 3.3$ °

$h = -14 \rightarrow 14$

$k = -12 \rightarrow 12$

$l = -10 \rightarrow 10$

8746 measured reflections

Refinement

Refinement on F^2

Least-squares matrix: full

$R[F^2 > 2\sigma(F^2)] = 0.053$

$wR(F^2) = 0.161$

$S = 1.12$

4791 reflections

179 parameters

22 restraints

Primary atom site location: structure-invariant

direct methods

Hydrogen site location: difference Fourier map

Only H-atom coordinates refined

$w = 1/[\sigma^2(F_o^2) + (0.094P)^2]$

where $P = (F_o^2 + 2F_c^2)/3$

$(\Delta/\sigma)_{\text{max}} < 0.001$

$\Delta\rho_{\text{max}} = 0.36$ e Å⁻³

$\Delta\rho_{\text{min}} = -0.43$ e Å⁻³

Absolute structure: Flack x determined using

647 quotients $[(I^+)-(I^-)]/[(I^+)+(I^-)]$ (Parsons *et al.*, 2013)

Absolute structure parameter: 0.43 (13)

Special details

Geometry. All esds (except the esd in the dihedral angle between two l.s. planes) are estimated using the full covariance matrix. The cell esds are taken into account individually in the estimation of esds in distances, angles and torsion angles; correlations between esds in cell parameters are only used when they are defined by crystal symmetry. An approximate (isotropic) treatment of cell esds is used for estimating esds involving l.s. planes.

Refinement. Refined as a 2-component twin

Fractional atomic coordinates and isotropic or equivalent isotropic displacement parameters (\AA^2)

	<i>x</i>	<i>y</i>	<i>z</i>	$U_{\text{iso}}^*/U_{\text{eq}}$
Mg1	0.4801 (4)	0.1376 (3)	0.5771 (6)	0.0178 (9)
Mg2	0.4708 (3)	0.1837 (4)	0.9931 (5)	0.0182 (10)
Cl1	0.1825 (3)	0.9715 (3)	0.5763 (4)	0.0262 (9)
Cl2	0.2944 (3)	0.5078 (3)	0.0497 (4)	0.0249 (8)
C1	0.4795 (10)	0.0190 (12)	0.2714 (13)	0.017 (3)
O1	0.4661 (9)	0.2884 (9)	1.1718 (12)	0.028 (2)
H1B	0.419 (11)	0.341 (10)	1.152 (18)	0.034*
H1A	0.468 (13)	0.250 (11)	1.247 (14)	0.034*
O2	0.4771 (7)	0.0395 (8)	1.1333 (10)	0.0196 (19)
O3	0.6440 (9)	0.1968 (9)	1.1050 (12)	0.028 (2)
H3B	0.680 (13)	0.211 (16)	1.203 (6)	0.034*
H3A	0.688 (12)	0.153 (13)	1.09 (2)	0.034*
O4	0.2896 (8)	0.1586 (9)	0.8686 (11)	0.025 (2)
H4B	0.264 (12)	0.148 (13)	0.932 (14)	0.029*
H4A	0.255 (12)	0.112 (11)	0.792 (12)	0.029*
O5	0.4634 (9)	0.3447 (9)	0.8750 (12)	0.029 (2)
H5A	0.433 (12)	0.371 (12)	0.781 (7)	0.034*
H5B	0.509 (12)	0.395 (10)	0.933 (13)	0.034*
O6	0.4774 (8)	0.0931 (8)	0.8055 (12)	0.0184 (19)
O7	0.4802 (9)	0.3153 (9)	0.5418 (13)	0.028 (2)
H7A	0.427 (8)	0.361 (9)	0.52 (2)	0.034*
H7B	0.536 (7)	0.358 (10)	0.57 (2)	0.034*
O8	0.6599 (8)	0.1449 (9)	0.7010 (12)	0.025 (2)
H8B	0.694 (12)	0.111 (12)	0.790 (8)	0.029*
H8A	0.686 (11)	0.116 (12)	0.645 (12)	0.029*
O9	0.4820 (8)	0.1034 (8)	0.3651 (11)	0.022 (2)
O10	0.3036 (8)	0.1571 (9)	0.4583 (11)	0.024 (2)
H10B	0.278 (11)	0.150 (13)	0.359 (5)	0.029*
H10A	0.262 (10)	0.117 (12)	0.481 (14)	0.029*

Atomic displacement parameters (\AA^2)

	U^{11}	U^{22}	U^{33}	U^{12}	U^{13}	U^{23}
Mg1	0.023 (2)	0.017 (2)	0.0156 (18)	−0.0018 (19)	0.0114 (15)	−0.004 (2)
Mg2	0.022 (2)	0.019 (2)	0.0152 (18)	0.0026 (17)	0.0102 (16)	0.0000 (17)
Cl1	0.0248 (16)	0.0273 (19)	0.0302 (17)	−0.0052 (14)	0.0162 (14)	−0.0031 (15)
Cl2	0.0242 (15)	0.0255 (16)	0.0257 (15)	0.0023 (14)	0.0126 (12)	0.0018 (14)
C1	0.021 (6)	0.023 (8)	0.010 (7)	0.001 (5)	0.008 (6)	−0.009 (6)

O1	0.048 (6)	0.021 (5)	0.024 (5)	0.008 (4)	0.023 (5)	0.009 (4)
O2	0.027 (5)	0.017 (5)	0.017 (4)	0.005 (4)	0.013 (4)	-0.003 (4)
O3	0.030 (6)	0.032 (6)	0.023 (5)	0.005 (4)	0.013 (5)	-0.001 (4)
O4	0.028 (5)	0.030 (5)	0.017 (5)	-0.002 (4)	0.012 (4)	0.001 (4)
O5	0.040 (6)	0.023 (5)	0.020 (5)	-0.006 (4)	0.013 (4)	-0.001 (4)
O6	0.025 (5)	0.016 (5)	0.017 (4)	0.000 (4)	0.012 (4)	0.002 (4)
O7	0.030 (5)	0.022 (5)	0.038 (7)	0.006 (4)	0.021 (5)	0.004 (4)
O8	0.024 (5)	0.029 (5)	0.020 (5)	0.003 (4)	0.010 (4)	-0.003 (4)
O9	0.034 (6)	0.018 (5)	0.020 (5)	0.002 (4)	0.018 (4)	0.005 (4)
O10	0.025 (5)	0.029 (6)	0.019 (5)	0.001 (4)	0.012 (4)	0.002 (4)

Geometric parameters (Å, °)

Mg1—O9	2.014 (10)	Mg2—O2	2.055 (10)
Mg1—O7	2.028 (11)	Mg2—O1	2.058 (11)
Mg1—O2 ⁱ	2.066 (9)	Mg2—O5	2.095 (11)
Mg1—O10	2.079 (11)	Mg2—O4	2.140 (11)
Mg1—O8	2.107 (11)	C1—O9	1.277 (15)
Mg1—O6	2.192 (10)	C1—O2 ⁱⁱ	1.285 (15)
Mg2—O3	2.036 (11)	C1—O6 ⁱ	1.305 (17)
Mg2—O6	2.054 (11)		
O9—Mg1—O7	91.7 (4)	O3—Mg2—O1	91.0 (5)
O9—Mg1—O2 ⁱ	94.2 (4)	O6—Mg2—O1	174.8 (5)
O7—Mg1—O2 ⁱ	174.1 (5)	O2—Mg2—O1	87.3 (4)
O9—Mg1—O10	92.8 (4)	O3—Mg2—O5	87.6 (4)
O7—Mg1—O10	84.2 (4)	O6—Mg2—O5	89.9 (4)
O2 ⁱ —Mg1—O10	94.6 (4)	O2—Mg2—O5	172.2 (4)
O9—Mg1—O8	89.5 (4)	O1—Mg2—O5	85.0 (4)
O7—Mg1—O8	87.7 (4)	O3—Mg2—O4	176.1 (5)
O2 ⁱ —Mg1—O8	93.2 (4)	O6—Mg2—O4	88.7 (4)
O10—Mg1—O8	171.6 (4)	O2—Mg2—O4	85.8 (4)
O9—Mg1—O6	155.8 (4)	O1—Mg2—O4	92.5 (5)
O7—Mg1—O6	112.5 (4)	O5—Mg2—O4	94.4 (4)
O2 ⁱ —Mg1—O6	61.6 (4)	O3—Mg2—Mg1 ⁱⁱⁱ	92.8 (3)
O10—Mg1—O6	89.6 (4)	O6—Mg2—Mg1 ⁱⁱⁱ	71.4 (3)
O8—Mg1—O6	91.6 (4)	O2—Mg2—Mg1 ⁱⁱⁱ	26.5 (3)
O9—Mg1—C1 ⁱⁱⁱ	124.7 (4)	O1—Mg2—Mg1 ⁱⁱⁱ	113.8 (3)
O7—Mg1—C1 ⁱⁱⁱ	143.6 (5)	O5—Mg2—Mg1 ⁱⁱⁱ	161.2 (3)
O2 ⁱ —Mg1—C1 ⁱⁱⁱ	30.5 (4)	O4—Mg2—Mg1 ⁱⁱⁱ	84.2 (3)
O10—Mg1—C1 ⁱⁱⁱ	93.4 (4)	O9—C1—O2 ⁱⁱ	121.5 (12)
O8—Mg1—C1 ⁱⁱⁱ	92.0 (4)	O9—C1—O6 ⁱ	123.5 (10)
O6—Mg1—C1 ⁱⁱⁱ	31.1 (4)	O2 ⁱⁱ —C1—O6 ⁱ	115.0 (10)
O9—Mg1—Mg2 ⁱ	67.8 (3)	O9—C1—Mg1 ⁱ	175.9 (10)
O7—Mg1—Mg2 ⁱ	159.4 (3)	O2 ⁱⁱ —C1—Mg1 ⁱ	54.7 (6)
O2 ⁱ —Mg1—Mg2 ⁱ	26.4 (2)	O6 ⁱ —C1—Mg1 ⁱ	60.3 (6)
O10—Mg1—Mg2 ⁱ	94.5 (3)	C1 ^{iv} —O2—Mg2	138.1 (8)
O8—Mg1—Mg2 ⁱ	93.9 (3)	C1 ^{iv} —O2—Mg1 ⁱⁱⁱ	94.7 (8)

O6—Mg1—Mg2 ⁱ	88.0 (3)	Mg2—O2—Mg1 ⁱⁱⁱ	127.1 (4)
C1 ⁱⁱⁱ —Mg1—Mg2 ⁱ	56.9 (3)	C1 ⁱⁱⁱ —O6—Mg2	134.5 (8)
O3—Mg2—O6	87.9 (4)	C1 ⁱⁱⁱ —O6—Mg1	88.5 (7)
O3—Mg2—O2	92.6 (4)	Mg2—O6—Mg1	137.0 (5)
O6—Mg2—O2	97.9 (4)	C1—O9—Mg1	142.8 (8)

Symmetry codes: (i) $x, -y, z-1/2$; (ii) $x, y, z-1$; (iii) $x, -y, z+1/2$; (iv) $x, y, z+1$.

Hydrogen-bond geometry (\AA , $^\circ$)

$D-H\cdots A$	$D-H$	$H\cdots A$	$D\cdots A$	$D-H\cdots A$
O1—H1A \cdots O9 ^{iv}	0.82 (3)	1.94 (6)	2.688 (14)	153 (13)
O1—H1B \cdots C12 ^{iv}	0.82 (3)	2.38 (4)	3.186 (11)	167 (12)
O3—H3A \cdots C12 ^v	0.82 (3)	2.32 (3)	3.135 (11)	174 (17)
O3—H3B \cdots O4 ^{vi}	0.82 (3)	2.10 (11)	2.796 (13)	143 (17)
O4—H4A \cdots C11 ^{vii}	0.82 (3)	2.36 (3)	3.176 (10)	171 (14)
O4—H4B \cdots C11 ^{viii}	0.82 (3)	2.49 (7)	3.251 (10)	155 (13)
O5—H5A \cdots C12 ^{viii}	0.82 (3)	2.45 (7)	3.222 (11)	157 (16)
O5—H5B \cdots C11 ^{ix}	0.81 (3)	2.54 (6)	3.327 (11)	164 (17)
O7—H7A \cdots C12 ^{viii}	0.82 (3)	2.42 (6)	3.212 (11)	163 (16)
O7—H7B \cdots C11 ^x	0.82 (3)	2.30 (4)	3.111 (11)	169 (16)
O8—H8A \cdots C12 ^{vi}	0.82 (3)	2.46 (5)	3.254 (10)	163 (11)
O8—H8B \cdots C12 ^v	0.82 (3)	2.41 (3)	3.233 (10)	178 (11)
O10—H10A \cdots C11 ^{vii}	0.82 (3)	2.34 (5)	3.146 (10)	166 (15)
O10—H10B \cdots C11 ^{xi}	0.82 (3)	2.67 (7)	3.424 (10)	154 (12)

Symmetry codes: (iv) $x, y, z+1$; (v) $x+1/2, y-1/2, z+1$; (vi) $x+1/2, -y+1/2, z+1/2$; (vii) $x, y-1, z$; (viii) $x, -y+1, z+1/2$; (ix) $x+1/2, -y+3/2, z+1/2$; (x) $x+1/2, y-1/2, z$; (xi) $x, -y+1, z-1/2$.